

Adiabatic loading of one-dimensional $SU(N)$ alkaline earth fermions in optical lattices

Lars Bonnes,¹ Kaden R. A. Hazzard,² Salvatore R. Manmana,² Ana Maria Rey,² and Stefan Wessel³

¹*Institute for Theoretical Physics, University of Innsbruck, A-6020 Innsbruck, Austria.**

²*JILA, NIST and University of Colorado, and Department of Physics, University of Colorado, Boulder, Colorado 80309-0440, USA.*

³*Institute for Theoretical Solid State Physics, JARA-FIT, and JARA-HPC, RWTH Aachen University, Otto-Blumenthal-Str. 26, D-52056 Aachen, Germany.*

(Dated: October 20, 2021)

Ultracold fermionic alkaline earth atoms confined in optical lattices realize Hubbard models with internal $SU(N)$ symmetries, where N can be as large as ten. Such systems are expected to harbor exotic magnetic physics at temperatures below the superexchange energy scale. Employing quantum Monte Carlo simulations to access the low-temperature regime of one-dimensional chains, we show that after adiabatically loading a weakly interacting gas into the strongly interacting regime of an optical lattice, the final temperature decreases with increasing N . Furthermore, we estimate the temperature scale required to probe correlations associated with low-temperature $SU(N)$ magnetism. Our findings are encouraging for the exploration of exotic large- N magnetic states in ongoing experiments.

PACS numbers: 67.85.-d, 03.75.Ss, 37.10.Jk

Ultracold fermionic alkaline earth atoms confined in optical lattices realize an important, tunable generalization of the Hubbard model, widely used to model strongly correlated electrons [1–5]. Within this generalization, the conventional spin-1/2 $SU(2)$ symmetry is enhanced to an $SU(N)$ symmetry. $N = 2I + 1$ is determined by the nuclear spin, I , which varies in alkaline earths from $I = 1/2$ to $I = 9/2$ depending on the atomic species. The $SU(N)$ symmetry arises because the electronic degrees of freedom have neither spin nor orbital angular momentum (due to the closed-shell structure) and thus decouple from the nuclear spin. In the electronic ground state the symmetry has been theoretically predicted to hold to an accuracy of 10^{-9} [1] and experiments have constrained deviations to be less than 5×10^{-4} [6]. Despite the large I , quantum fluctuations remain important due to the enhanced symmetry, giving rise to magnetic frustration and exotic ground states, such as valence-bond solids [7–11], exotic spin orderings [12] or (chiral) spin liquids [13, 14] in addition to the plethora of potential phases for the conventional $N = 2$ Hubbard model, such as antiferromagnets, d-wave superconductors, and nematic states. The possibility of mimicking such exciting many-body physics, as well as potential applications to atomic clocks [15–18], measurements of fundamental constants [19], and quantum information processing [20], has stimulated substantial experimental progress [4, 21–30].

Although cold atom experiments routinely reach nanokelvin temperatures, it is an ongoing effort to achieve temperatures and entropies sufficiently low to see superexchange driven magnetic many-body physics [5, 31–33]. Hazzard *et al.* showed via a high temperature series expansion (HTSE) that for final temperatures $T \gtrsim t$, with t the tunneling rate in the lattice, the temperatures

reached after adiabatic loading from experimentally realistic initial conditions decreases with increasing N [34]. Closely related is the finding that the entropy of Mott states increases with N even faster than the initial weakly interacting gas entropy. The question of the behavior below t , and especially below the magnetic exchange energy scale $J \sim t^2/U$ where U is the on-site interaction, has remained open even though this is one relevant for exploring exotic $SU(N)$ magnetism. Two issues are particularly relevant in this regime: how does N affect (i) the temperature reached by adiabatic loading and (ii) the physical properties, such as correlation functions?

Here, we address both questions in one dimensional systems using quantum Monte Carlo calculations. We show that also for $T < t^2/U$ the temperatures reached by adiabatic loading decrease with increasing N . This decrease occurs even relative to the temperature scales of interesting physics, for example the onset of Luttinger liquid behavior, magnetic correlations, or ground state-like correlations.

The Hamiltonian of the $SU(N)$ Hubbard model describing alkaline earth atoms in optical lattices is [1]

$$\mathcal{H} = -t \sum_{i,\alpha} \left(f_{\alpha,i}^\dagger f_{\alpha,i+1} + \text{H.c.} \right) + \frac{U}{2} \sum_{i,\alpha \neq \beta} n_i^\alpha n_i^\beta, \quad (1)$$

where $f_{\alpha,i}^\dagger$ ($f_{\alpha,i}$) are creation (annihilation) operators for fermions of flavor α at site i , and $n_i^\alpha = f_{\alpha,i}^\dagger f_{\alpha,i}$. At filling $1/N$ (density $n = 1$) local moment (Heisenberg) quantum magnetism arises in the strong interaction limit, where second order processes lead to a flavor exchange interaction scale $J \sim t^2/U$. We employ quantum Monte-Carlo (QMC) to obtain the low temperature thermodynamic properties of one-dimensional lattice alkaline earth atoms described by Eq. (1) in the relevant regime $T \ll t \ll U$,

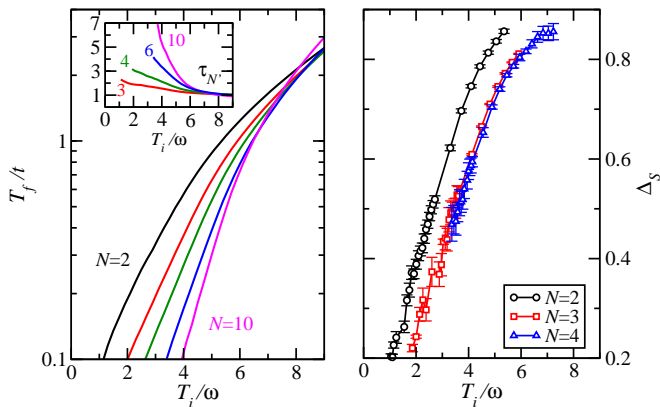


FIG. 1: (Color online) *Left*: Final vs. initial temperature for the adiabatic loading scheme for $N = 2, 3, 4, 6$ and 10 (from left to right) inside a harmonic trap with trap frequency $\omega = 2\pi \times 90\text{Hz}$ and for $U/t = 8$. One can alternatively translate the initial temperature into units of Fermi temperature T_F , using $T_i/T_F = \{2.8, 3.2, 3.5, 4.1, 4.8\} \times 10^{-2}(T_i/\omega)$ for $N = \{2, 3, 4, 6, 10\}$. The inset shows the temperature decrease relative to the $N = 2$ Hubbard model, $\tau_{N'} = T_f(N = 2)/T_f(N = N')$, for (from bottom to top) $N' = 3$ (red), $N' = 4$ (green), $N' = 6$ (blue) and $N' = 10$ (magenta) vs. T_i/ω . *Right*: Distance measure Δ_S of the magnetic correlations relative to the ground state values for a homogeneous system with $U/t = 8$ at $n = 1$.

much lower than the temperature scales accessible within the HTSE.

These thermodynamic properties allow us to calculate the temperatures that experiments can achieve using the standard experimental adiabatic lattice loading protocol: the systems are prepared by starting with a weakly interacting gas and slowly turning on the lattice [32, 33]. Ideally, this is done sufficiently slowly to maintain adiabaticity, minimizing the increase in entropy. The final temperature in the adiabatic limit in this sense provides a lower bound to the experimentally achievable temperatures, and in practice the adiabatic bound is frequently an accurate approximation [32, 33, 35].

In the following, we consider loading a three dimensional ($d = 3$) trapped gas (no lattice) into a two dimensional array of independent one dimensional lattices. Fig. 1 (left panel) shows our central result, the final temperature T_f of the harmonically trapped lattice system with fixed trapping frequency ω as a function of the initial temperature T_i before applying the lattice [36]. We use realistic experimental particle number and trap frequencies, similar to Ref. [34]: $\mathcal{N} = 1.5 \times 10^4$ and $\omega = 2\pi \times 90\text{Hz}$. For loading ^{173}Yb in a 266 nm lattice, our choice of U corresponds to the lattice depth required to obtain $U/t = 8$. We observe from Fig. 1 that the final temperature achieved for $T_i/\omega < 9$ significantly decreases with increasing N . This includes the lowest temperatures, an order of magnitude lower than

where the HTSE is applicable, and is encouraging for experimentally achieving $\text{SU}(N)$ quantum magnetism. For instance, at the relatively warm temperature $T_i/\omega = 4$ (some experiments are already at even lower temperatures) the final temperature is already decreased by factors of 1.7 ($N = 3$), 1.85 ($N = 4$), 3.25 ($N = 6$) and 5.6 ($N = 10$) compared to the conventional $N = 2$ case. We note that even this is a pessimistic estimate since these ratios compare different N fixing T_i/ω . Experimentally, T_i will likely decrease with N , as discussed in Ref. 34. The reason why T_f decreases with N , for fixed initial T_i , is the scaling of the initial and final states' entropy with N . At very low temperature $T \ll t^2/U$, the Mott insulator possesses $N - 1$ gapless channels, and the metal possesses N [37, 38]. The increasing number of gapless excitations implies that the entropy growth at fixed temperature is faster than the initial state's $N^{1/3}$. Thus, the final temperatures will decrease with increasing N . This is even more favorable than at high temperatures $T \gtrsim t$, where the Mott insulator accommodates an entropy $S \sim \log N$ [34], as can be seen in Fig. 1. However, even for $T > t$, for $N \lesssim 20$ the logarithmic term grows *fast* enough to compensate for the $N^{1/3}$ in the initial state, leading to colder final states with increasing N .

The enhanced cooling effect has indeed been observed (at elevated temperatures) for $\text{SU}(6)$ fermions in recent experiments on a ^{173}Yb gas in a three-dimensional optical lattice [39]. In particular, their findings are in good agreement with the HTSE results (valid for their experiments), confirming the validity of the adiabaticity assumption for their experiments.

We now describe the procedure used to obtain Fig. 1. Assuming adiabaticity, the initial temperature T_i and particle number \mathcal{N}_i in the absence of the lattice uniquely determine the final temperature T_f through the conservation of entropy and particle number. T_f can be calculated in terms of the experimentally measurable T_i and \mathcal{N}_i once one knows how the particle number and entropy of the system in a lattice depend on temperature T and the chemical potential μ , $\mathcal{N}_f(T, \mu)$ and $S_f(T, \mu)$, as follows: We calculate T_f and μ_f by solving particle number and entropy conservation equations, $\mathcal{N}_f(T_f, \mu_f) = \mathcal{N}_i(T_i, \mu_i)$ and $S_f(T_f, \mu_f) = S_i(T_i, \mu_i)$, for T_f and μ_f in terms of the initial temperature T_i and chemical potential μ_i of the weakly interacting gas. In practice, since experimentalists measure the initial particle number \mathcal{N}_i rather than μ_i , we solve for μ_i in terms of T_i and \mathcal{N}_i using $\mathcal{N}_i(\mu_i, T_i) = \mathcal{N}_i$. The conservation equations become

$$\mathcal{N}_f(T_f, \mu_f) = \mathcal{N}_i, \quad S_f(T_f, \mu_f) = S_i(T_i, \mu_i(\mathcal{N}_i, T_i)). \quad (2)$$

The functions $\mathcal{N}_i(T, \mu)$ and $S_i(T, \mu)$ are those of a gas in a harmonic trapping potential $V(r) = m\omega^2 r^2/2$. For relevant experimental initial conditions, the temperature is low compared to the Fermi temperature, interactions are weak, and the number of particles is large, so the

semiclassical approximation to the non-interacting degenerate Fermi gas is accurate, giving [34] $\mathcal{N}_i(\mu, T) = (N/d!)(\mu/\omega)^d$ and $S_i(\mu, T) = \frac{T_i}{\omega} \frac{N\pi^2}{3^{(d-1)!}} (\frac{\mu}{\omega})^{d-1}$. We consider dimension $d = 3$.

We obtain the functions $\mathcal{N}_f(T, \mu)$ and $S_f(T, \mu)$ in two steps. First, to compute the total particle and entropy in the trap we apply the local density approximation (LDA) [40]: we obtain the properties at position \mathbf{r} from those of a homogeneous system at a chemical potential $\mu(\mathbf{r}) = \mu - V(\mathbf{r})$. Due to the large particle number (about 30 particles in the central tube at $T = 0$), this approximation will be accurate. Second, to obtain the homogeneous system properties used in the LDA, we use sign-problem-free QMC simulations [41] within the stochastic series expansion (SSE) framework [42–44]. We first calculate the density and entropy for finite systems up to $L = 100$ sites, with open boundaries within the grand-canonical ensemble for various values of the chemical potential μ . We find finite size effects to be negligible on these lattice sizes for the quantities of interest below. The entropy is obtained by a standard thermodynamic integration of the energy E . In fact, the HTSE agrees well with the QMC data down to $T/t \approx 2$, as illustrated in Fig. 2, and we thus used the HTSE results at $T/t = 10$ as the high-temperature end point for the thermodynamic integration. Increasingly dense temperature grids are required to perform this integration down to lower temperatures, and we were able to perform this procedure down to $T/t = 0.1$. We find that our data indeed connects to the $T \rightarrow 0$ limit, where S scales linear in T [37]. We finally compared our QMC results to ground state properties [38], obtained using the density matrix renormalization group (DMRG) [45–48]. In particular, the extrapolated ground state energies agree with DMRG results within the statistical error bars. Finally, we calculate tables of \mathcal{N}_f and S_f for a dense grid of μ and T , construct interpolating functions of this data supplemented, for very negative μ , with the virial expansion that accurately describes the gas in this regime. The adiabatic loading equations Eqs. (2) are then solved numerically to obtain the results in Fig. 1.

Having determined achievable temperatures, we next turn to correlation functions that are indicative for low-energy $SU(N)$ magnetism in these systems. The relevant spin-spin correlation function is related to the equal and unequal flavor density-density correlation functions [38]

$$\mathcal{S}(|i-j|) = \frac{1}{N} \sum_{\alpha} \langle n_i^{\alpha} n_j^{\alpha} \rangle - \frac{1}{N(N-1)} \sum_{\alpha \neq \beta} \langle n_i^{\alpha} n_j^{\beta} \rangle. \quad (3)$$

This can be measured via, for example, Bragg spectroscopy [49]. To compare finite-temperature and ground state correlations (obtained from DMRG), we define an appropriate distance measure that accounts also for the

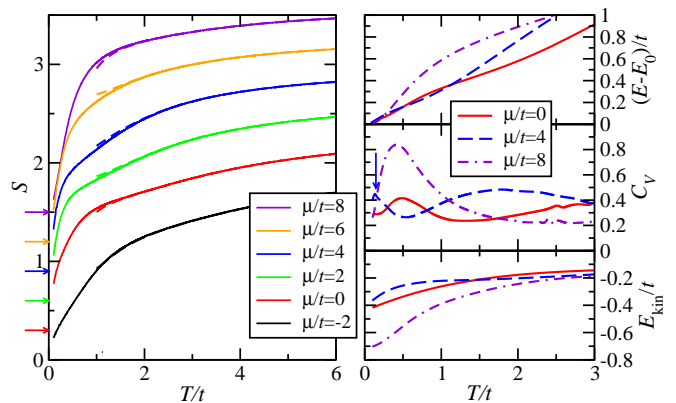


FIG. 2: (Color online) *Left*: Entropy S per site for $N = 3$, $U/t = 8$ at fixed chemical potentials from $\mu/t = -2$ (bottom) to $\mu/t = 8$ (top) obtained from QMC for a homogeneous system. We note, that the system forms a Mott insulating ground state with density $n = 1$ for $\mu/t \approx 1.5$ to 5 . Dashed lines down to $T/t = 1$ denote HTSE results from Ref. 34. For clarity, an offset was added to the entropies, indicated by the arrows. *Right top*: Temperature dependence of the energy per site E relative to the extrapolated ground state energy E_0 , from QMC. *Right middle*: Temperature dependence of the specific heat C_V [54]. The arrow indicates the low- T peak in C_V in the Mott regime. *Right bottom*: Temperature dependence of the kinetic energy E_{kin} , from QMC. Statistical errors are below the line width.

overall magnitude of the ground state correlations [38],

$$\Delta_{\mathcal{S}}(T) = \frac{\sqrt{\sum_{r=1}^L (\mathcal{S}(r, T) - \mathcal{S}(r)_{\text{DMRG}})^2}}{\sqrt{\sum_{r=1}^L \mathcal{S}(r)_{\text{DMRG}}^2}}. \quad (4)$$

This quantity is sensitive to both long range and short range magnetic correlations [50, 51]. The right panel of Fig. 1 shows $\Delta_{\mathcal{S}}$ for $n = 1$ and $U/t = 8$ as a function of T_i/ω , using T_f/t determined from the lattice loading [52]. This shows that increasing N brings the system not only to lower values of T , but also into a region where ground-state-like correlations are more developed.

A hallmark of quantum magnetism in N -component Luttinger liquids (LL) are $2k_F = 2\pi n/N$ oscillations in the spin correlation functions, with n the density [38, 53]. Figure 3 shows the spin structure factor $\tilde{\mathcal{S}}(k)$, the Fourier transformation of $\mathcal{S}(r)$, for $N = 3$ and 4 at $U/t = 8$ and fixed filling of $1/N$ ($n = 1$). At low temperatures $T/t \lesssim 0.1$, the $2k_F$ peak appears, as expected from LL theory. This is associated with a maximum in the specific heat C_V [54] shown in Fig. 2, marking the onset of $SU(N)$ Heisenberg physics [55]. At high temperatures $T/t \gtrsim 1$, $\tilde{\mathcal{S}}(k)$ instead becomes featureless. However, in an intermediate regime $0.5 \lesssim T/t \lesssim 1$, a broad peak at $k = \pi$ is observed, which shifts towards $2k_F$ as the temperature is lowered towards $T \approx t^2/U$: at these temperatures, nearest neighbor correlations emerge. While this

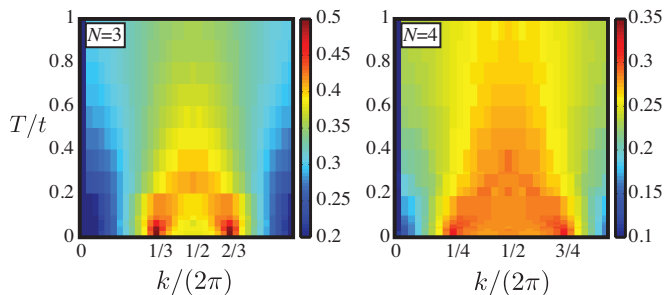


FIG. 3: (Color online) Spin structure factor $\tilde{S}(k)$ for a homogeneous system with density $n = 1$ for $N = 3$ (left) and 4 (right), $U/t = 8$ as a function of the final temperature T/t (here, $L = 48$). The characteristic $2k_F$ peaks below $T/t \approx 0.15$ signal the onset of magnetic correlations.

regime is not representative for the ground state behavior, the short-ranged magnetic correlations determine the main features of the structure factors, and experiments reaching this temperature regime should be able to investigate magnetic behavior. In Fig. 2, the entropy and kinetic energy similarly display the onset of the magnetic exchange region as a kink and large decrease, respectively. This happens around $T/t \approx 0.5$. For $N = 2$, we have checked that our data are consistent with former studies of the SU(2) Hubbard model [55, 56].

For intermediate temperature $t^2/U \ll T \ll t$, one can ask whether the system realizes a SU(N) generalization of the spin-incoherent Luttinger liquid (siLL) [57, 58] where the charge degrees of freedom show LL-like behaviour with a simultaneous absence of significant spin correlations. Here, we find no clear signatures of siLL in the density structure factor near $k = \pi n$ (not shown). We leave a more in-depth study for future work, where it will likely be beneficial to examine the momentum distribution $n(k)$, as was done for the SU(2) case [58].

Summary.— We studied the one-dimensional SU(N) Fermi-Hubbard model at finite temperatures employing numerically exact quantum Monte Carlo simulations. We calculated the density and entropy as functions of chemical potential and temperature and used this to determine final temperatures of the lattice system after adiabatically loading an optical lattice from a degenerate gas. We found substantial decreases of the final temperature with increasing N , even down to low temperatures $T \lesssim t^2/U \ll t$. Together with our results for the temperature dependence of correlation functions, we envisage that it should be possible to explore features of SU(N) quantum magnetism in ongoing experiments with alkaline earth atoms.

Acknowledgements

We acknowledge useful discussions with G. Chen and M. Hermele. This work was supported by the Austrian Ministry of Science BMWF as part of the UniInfrastrukturprogramm of the Forschungsplattform Scientific Computing at LFU Innsbruck, by the NSF-PIF and NSF-PFC grants, by the AFOSR and by the ARO with funding from the DARPA-OLE program. We also acknowledge allocation of CPU time from NIC Jülich where parts of the calculations were performed. KH thanks the NRC for support. KH also thanks the Aspen Center for Physics, which is supported by the NSF, for its hospitality while a portion of this work was carried out.

Note added.— Recently, Messio and Mila explored the N -dependence of the entropy and correlations in the Heisenberg limit of the SU(N) systems considered here [59]; their results are in accord with our finding for the Hubbard model, obtained at $U/t = 8$.

* Electronic address: lars.bonnes@uibk.ac.at

- [1] A. V. Gorshkov, M. Hermele, V. Gurarie, C. Xu, P. S. Julienne, J. Ye, P. Zoller, E. Demler, M. D. Lukin, and A. M. Rey, *Nature Physics* **6**, 289 (2010).
- [2] C. Wu, J.-p. Hu, and S.-c. Zhang, *Phys. Rev. Lett.* **91**, 186402 (2003).
- [3] M. A. Cazalilla, A. F. Ho, and M. Ueda, *New Journal of Physics* **11**, 103033 (2009).
- [4] T. Fukuhara, S. Sugawa, M. Sugimoto, S. Taie, and Y. Takahashi, *Phys. Rev. A* **79**, 041604 (2009).
- [5] S. Sugawa, K. Inaba, S. Taie, R. Yamazaki, M. Yamashita, and Y. Takahashi, *Nature Physics* **7**, 642 (2011).
- [6] S. Stellmer, R. Grimm, and F. Schreck, *Phys. Rev. A* **84**, 043611 (2011).
- [7] N. Read and S. Sachdev, *Phys. Rev. Lett.* **62**, 1694 (1989).
- [8] H. Nonne, E. Boulat, S. Capponi, and P. Lecheminant, *Mod. Phys. Lett. B* **25**, 955 (2011).
- [9] B. Bauer, P. Corboz, A. M. Läuchli, L. Messio, K. Penc, M. Troyer, and F. Mila, *Phys. Rev. B* **85**, 125116 (2012).
- [10] I. Affleck and J. B. Marston, *Phys. Rev. B* **37**, 3774 (1988).
- [11] C. Honerkamp and W. Hofstetter, *Phys. Rev. Lett.* **92**, 170403 (2004).
- [12] T. A. Tóth, A. M. Läuchli, F. Mila, and K. Penc, *Phys. Rev. Lett.* **105**, 265301 (2010).
- [13] M. Hermele, V. Gurarie, and A. M. Rey, *Phys. Rev. Lett.* **103**, 135301 (2009).
- [14] M. Hermele and V. Gurarie, *Phys. Rev. B* **84**, 174441 (2011).
- [15] T. Ido and H. Katori, *Phys. Rev. Lett.* **91**, 053001 (2003).
- [16] A. D. Ludlow, T. Zelevinsky, G. K. Campbell, S. Blatt, M. M. Boyd, M. H. G. de Miranda, M. J. Martin, J. W. Thomsen, S. M. Foreman, J. Ye, T. M. Fortier, J. E. Stalnaker, S. A. Diddams, Y. L. Coq, Z. W. Barber, N. Poli, N. D. Lemke, K. M. Beck, and C. W. Oates, *Science* **319**, 1805 (2008).

- [17] N. D. Lemke, A. D. Ludlow, Z. W. Barber, T. M. Fortier, S. A. Diddams, Y. Jiang, S. R. Jefferts, T. P. Heavner, T. E. Parker, and C. W. Oates, *Phys. Rev. Lett.* **103**, 063001 (2009).
- [18] A. Derevianko and H. Katori, *Rev. Mod. Phys.* **83**, 331 (2011).
- [19] S. Kotochigova, T. Zelevinsky, and J. Ye, *Phys. Rev. A* **79**, 012504 (2009).
- [20] A. Daley, *Quantum Information Processing* **10**, 865 (2011).
- [21] Y. Takasu, K. Maki, K. Komori, T. Takano, K. Honda, M. Kumakura, T. Yabuzaki, and Y. Takahashi, *Phys. Rev. Lett.* **91**, 040404 (2003).
- [22] T. Fukuhara, S. Sugawa, and Y. Takahashi, *Phys. Rev. A* **76**, 051604 (2007).
- [23] S. Kraft, F. Vogt, O. Appel, F. Riehle, and U. Sterr, *Phys. Rev. Lett.* **103**, 130401 (2009).
- [24] S. Stellmer, M. K. Tey, B. Huang, R. Grimm, and F. Schreck, *Phys. Rev. Lett.* **103**, 200401 (2009).
- [25] Y. N. M. de Escobar, P. G. Mickelson, M. Yan, B. J. DeSalvo, S. B. Nagel, and T. C. Killian, *Phys. Rev. Lett.* **103**, 200402 (2009).
- [26] P. G. Mickelson, Y. N. M. de Escobar, M. Yan, B. J. DeSalvo, and T. C. Killian, *Phys. Rev. A* **81**, 051601 (2010).
- [27] B. J. DeSalvo, M. Yan, P. G. Mickelson, Y. N. M. de Escobar, and T. C. Killian, *Phys. Rev. Lett.* **105**, 030402 (2010).
- [28] M. K. Tey, S. Stellmer, R. Grimm, and F. Schreck, *Phys. Rev. A* **82**, 011608 (2010).
- [29] S. Taie, Y. Takasu, S. Sugawa, R. Yamazaki, T. Tsujimoto, R. Murakami, and Y. Takahashi, *Phys. Rev. Lett.* **105**, 190401 (2010).
- [30] S. Stellmer, B. Pasquiou, R. Grimm, and F. Schreck, *arXiv:1205.4505v1* (2012).
- [31] D. C. McKay and B. DeMarco, *Reports on Progress in Physics* **74**, 054401 (2011).
- [32] R. Jördens, N. Strohmaier, K. Guenter, H. Moritz, and T. Esslinger, *Nature* **455**, 204 (2008).
- [33] U. Schneider, L. Hackermüller, S. Will, T. Best, I. Bloch, T. A. Costi, R. W. Helmes, D. Rasch, and A. Rosch, *Science* **322**, 1520 (2008).
- [34] K. R. A. Hazzard, V. Gurarie, M. Hermele, and A. M. Rey, *Phys. Rev. A* **85**, 041604 (2012).
- [35] S. S. Natu, K. R. A. Hazzard, and E. J. Mueller, *Phys. Rev. Lett.* **106**, 125301 (2011).
- [36] Fixed ω is the simplest choice. Depending on experimental details, ω can either increase or decrease in time, so staying constant is a fair compromise. Moreover, it may be accurate, since frequently the trapping frequency usually only changes by $\lesssim 20\%$. Finally, it is expected that the qualitative trends are unchanged by a lattice depth dependent ω . At least for $T \gtrsim t$, Ref. [34] showed explicitly that time-dependent ω had no effect on even the shape of T_f versus T_i , just on the absolute scale
- [37] K. Lee, *Physics Letters A* **187**, 112 (1994).
- [38] S. R. Manmana, K. R. A. Hazzard, G. Chen, A. E. Feiguin, and A. M. Rey, *Phys. Rev. A* **84**, 043601 (2011).
- [39] S. Taie, R. Yamazaki, S. Sugawa and Y. Takahashi, *arXiv:1208.4883v1*.
- [40] C. J. Pethick and H. Smith, *Bose-Einstein Condensation in Dilute Gases* (Cambridge University Press, Cambridge, 2002).
- [41] In the low-density wings of the trap, the physics is given by the virial expansion, so rather than extending the QMC deep into this trivial regime, we use the virial expansion for $\mu < -10t$.
- [42] A. W. Sandvik, *Phys. Rev. B* **59**, R14157 (1999).
- [43] O. F. Syljuåsen and A. W. Sandvik, *Phys. Rev. E* **66**, 046701 (2002).
- [44] F. Alet, S. Wessel, and M. Troyer, *Phys. Rev. E* **71**, 036706 (2005).
- [45] S. R. White, *Phys. Rev. Lett.* **69**, 2863 (1992).
- [46] S. R. White, *Phys. Rev. B* **48**, 10345 (1993).
- [47] *Density Matrix Renormalization - A New Numerical Method in Physics*, edited by I. Peschel, X. Wang, M. Kaulke, and K. Hallberg (Springer Verlag, Berlin, 1999).
- [48] U. Schollwöck, *Rev. Mod. Phys.* **77**, 259 (2005).
- [49] I. Carusotto, *J. Phys. B* **39**, S211 (2006).
- [50] D. Greif, L. Tarruell, T. Uehlinger, R. Jördens, and T. Esslinger, *Phys. Rev. Lett.* **106**, 145302 (2011).
- [51] E. V. Gorelik, D. Rost, T. Paiva, R. Scalettar, A. Klümper, and N. Blümer, *Phys. Rev. A* **85**, 061602 (2012).
- [52] Here, we are limited to $L = 48$ and $N \leq 4$ since the DMRG calculations suffer from a linear increase of the entanglement entropy with N [38, 60]. The suppression of the spin correlation functions with increasing N [38] leads to relatively large error bars in the calculations of Δ_S .
- [53] R. Assaraf, P. Azaria, M. Caffarel, and P. Lecheminant, *Phys. Rev. B* **60**, 2299 (1999).
- [54] The specific heat can be estimated directly by the energy fluctuations but its statistical noise is then very large in the low temperature regime. The data for the specific heat in Fig. 2 is thus obtained by numerical differentiation of the energy with respect to T using a spline interpolation.
- [55] N. Kawakami, T. Usuki, and A. Okiji, *Phys. Lett. A* **135**, 476 (1989).
- [56] A. W. Sandvik, *J. Phys. A* **25**, 3667 (1992).
- [57] G. A. Fiete, *Rev. Mod. Phys.* **79**, 801 (2007).
- [58] A. E. Feiguin and G. A. Fiete, *Phys. Rev. B* **81**, 075108 (2010).
- [59] L. Messio and F. Mila, *arXiv:1207.1320v1*.
- [60] M. Führinger, S. Rachel, R. Thomale, M. Greiter, and P. Schmitteckert, *Ann. Phys.* **17**, 922 (2008).